# Single-Junction Organic Solar Cells Based on a Novel Wide-Bandgap Polymer with Efficiency of 9.7%

*Lijun Huo, Tao Liu, Xiaobo Sun, Yunhao Cai, Alan J. Heeger, and Yanming Sun**

Organic bulk heterojunction (BHJ) solar cells comprising conjugated polymers and fullerene derivatives have recently attracted attention due to their lightweight, low cost, and the potential for the fabrication of large-area flexible devices. In the past few years, extensive effort has focused on developing donor–acceptor (D–A) conjugated polymers, leading to steady increases in power conversion efficiencies (PCEs). Recently, PCEs over 10% have been reported for both single and multi-junction organic solar cells.[1]

In terms of the development of D–A conjugated polymers, the emphasis has been on moderate-bandgap (MBG, $E_g$: 1.6–1.8 eV)[2] and low-bandgap (LBG, $E_g$ < 1.6 eV) copolymers.[3] A number of promising MBG and LBG copolymers with various monomer compositions, such as oligothienyl (oTh), benzodithiophene (BDT), benzothiadiazole (BT), thieno[3,4-b]thiophene (TT), diketopyrrolopyrrole (DPP), and indigo (IID) motifs, show high PCEs in the range of 8%–10%.[4,5] However, the design and synthesis of high performance wide-bandgap (WBG) polymers ($E_g$ > 1.8 eV) still remains a challenge.[6] Solar cells based on WBG polymers tend to have high open-circuit voltage ($V_{oc}$), but relatively low short-circuit current ($J_{sc}$), resulting in moderate PCEs.[7] To our best knowledge, the highest PCEs reported in the literature for WBG polymers, such as poly(3-hexylthiophene) (P3HT), poly[N-9″-hepta-decanyl-2,7-carbazole-alt-5,5-(4′,7′-di-2-thienyl-2′,1′,3′-benzothiadiazole)] (PCDTBT), and other WBG polymers are typically less than 9%.[4d,8]

Exploration of high-performance WBG polymers is of crucial importance for tandem (or multi-junction) organic solar cells. Tandem cells are the most promising route to reaching cell efficiencies up to 15%.[9] In a tandem solar cell, two subcells with complementary absorption spectra are stacked in series, in which the WBG polymers are used to convert shorter wavelength sunlight to electricity with a high open-circuit voltage.

In the search for ideal WBG building block candidates, BDT as one of the classical organic semiconducting units receives attention due to its high stability against oxidation ability and planar molecular framework.[10] However, most WBG polymers containing the BDT unit suffer from low short-circuit current.[7a,11] To overcome this problem, a new approach to enlarging π-conjugated system with fused aromatic rings has been recently reported.[12] Based on our previous research results, dithieno[2,3-d;2′,3′-d′]benzo[1,2-b;4,5-b′]dithiophene (DTBDT) with extended π-conjugation can effectively improve its charge carrier transport when compared to BDT.[12a,b] This is mainly attributed to its more planar molecular conformation, which can reduce conformational disorder of the backbone and increase molecular rigidity of the polymer in the solid state to facilitate electron delocalization. Similar observations have also been reported by several other groups.[13] For example, Geng and co-workers discovered when a carbazole unit is covalently bonded with two outer thiophenes to form the fused-ring dithienocarbazole, the PCEs can be significantly improved.[13b]

Inspired by the above ideas, we present a novel WBG copolymer, poly{dithieno[2,3-d:2′,3′-d′]benzo[1,2-b:4,5-b′]dithiophene-co-1,3-bis(thiophen-2-yl)-benzo-[1,2-c:4,5-c′]dithiophene-4,8-dione} (PDBT-T1) with energy gap, $E_g$ = 1.85 eV, which is composed of an electron-rich DTBDT subunit and a strong electron-deficient 1,3-bis(5-bromothiophen-2-yl)-5,7-bis(2-ethylhexyl)-4H,8H-benzo[1,2-c:4,5-c′]dithiophene-4,8-dione (T1) subunit. The polymer has a highly rigid backbone since both DTBDT and T1 subunits are rigid and planar. Single-junction organic solar cells based on PDBT-T1 as the donor and [6,6]-phenyl $C_{71}$-butyric acid methyl ester ($PC_{70}BM$) as the acceptor have been fabricated. A high PCE of 8.3% was achieved for cells without any solvent additives and post-annealing treatments. When 1,8-diiodooctane (DIO) was used as the solvent additive, the PCE can be further improved to 9.7%, with a high fill factor (*FF*) of 75%. To the best of our knowledge, this efficiency represents the highest values reported in the literature so far for single-junction organic solar cell based on WBG polymers.

The synthetic route of PDBT-T1 is illustrated in **Scheme 1**. Dialkylthieno-2-yl flanked dithieno[2,3-d:2′,3′-d′]benzo[1,2-b:4,5-b′]dithiophene subunit was first prepared according to our previous reported approach.[12b] Branched 2-ethylhexyl was linked to T1 acceptor subunit afterward.[14] The bis(trimethyltin)-DTBDT monomer was prepared with the similar method as used in the synthesis of thienyl-substituted BDT derivatives. PDBT-T1 was prepared through the typical Stille coupling reaction between the bis(trimethyltin) monomer (DBT) and T1. PDBT-T1 exhibits moderate solubility in toluene or xylenes, but good solubility in chloroform ($CHCl_3$) and *o*-dichlorobenzene (*o*-DCB) at room temperature. The polymer is thermally stable with a decomposition temperature beyond 315 °C under inert atmosphere (Figure S1, Supporting Information). No thermal transitions were observed from differential scanning calorimetry (DSC) measurements.

Prof. L. Huo, T. Liu, Prof. X. Sun, Y. Cai, Prof. Y. Sun
Key Laboratory of Bio-Inspired Smart Interfacial Science and Technology of Ministry of Education
Beijing Key Laboratory of Bio-Inspired Energy Materials and Devices
School of Chemistry and Environment
Beihang University
Beijing 100191, P. R. China
E-mail: sunym@buaa.edu.cn
Prof. L. Huo, T. Liu, Prof. X. Sun, Y. Cai, Prof. A. J. Heeger, Prof. Y. Sun
Heeger Beijing Research and Development Center
International Research Institute for Multidisciplinary Science
Beihang University
Beijing 100191, P. R. China

DOI: 10.1002/adma.201500647

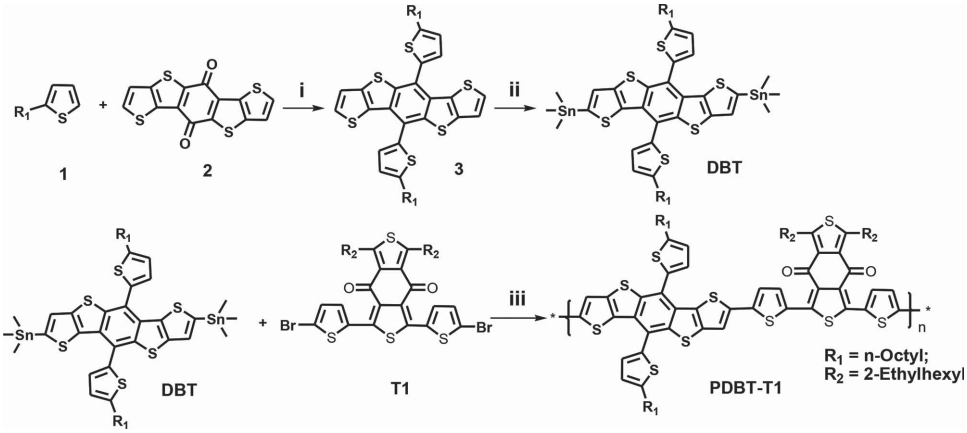


**Scheme 1.** Chemical structures of DBT, T1, and PDBT-T1, and synthetic procedure of PDBT-T1: i) *n*-butyllithium, THF, inert atmosphere, 50 °C, 1.5 h; then $SnCl_2$, $HCl/H_2O$, inert atmosphere, 50 °C, 1.5 h; ii) *n*-butyllithium, THF, inert atmosphere, –78 °C, 1 h, then trimethyltin chloride, inert atmosphere, ambient temperature, 1 h; iii) $Pd(PPh_3)_4$, Toluene/DMF, inert atmosphere, reflux, 8 h.

Theoretical calculations were performed by using the density functional theory (DFT) with the B3LYP/6–31G (d,p) basis set. To simply the calculation, alkyl chains were ignored. As illustrated Figure S2, Supporting Information, the highest occupied molecular orbital (HOMO) surface of the polymer is delocalized on both DTBDT and T1 units. However, the lowest unoccupied molecular orbital (LUMO) surface of the polymer is more localized on the acceptor unit, indicating that the T1 unit exhibit strong electron withdrawing effect. Meanwhile, the polymeric backbone exhibits good linear conformations, as well as a dominated continuous positive electrostatic potential (ESP), which are favorable to get high carrier mobility (**Figure 1**).

The UV–vis absorption spectra of PDBT-T1 in diluted $CHCl_3$ solution and thin film are shown in **Figure 2**a. PDBT-T1 exhibits two well-defined absorption peaks, one at higher energies (300–450 nm) resulting from $\pi$–$\pi^*$ transitions and the other one at lower energies (500–700 nm). The thin-film absorption of PDBT-T1 exhibits similar optical property to that in solution. The maximum absorption peak is at 620 nm for PDBT-T1 in solution, while the peak is at 628 nm in thin film with a slight redshift. In addition, obvious vibronic shoulder peaks at lower energies are observed both in solution and thin film, which suggests significant order in the polymer structure. The results indicate that polymer chains in solution already exist in very strong aggregation. Similar results were reported for other conjugated polymers with extended fused rings.[13b,15] The optical bandgap ($E_g^{opt}$) estimated from the film absorption onset is 1.85 eV. Electrochemical cyclic voltammetry (CV) was used to investigate the energy levels (Figure 2b). The HOMO and the LUMO levels calculated from the onset of oxidation and reduction potentials are –5.36 and –3.43 eV, respectively. Thus, the electrochemical bandgap of PDBT-T1 is estimated to be about 1.93 eV, in good agreement with the optical bandgap. The deep HOMO value around –5.36 eV is one of the encouraging characteristics for a donor material. Thus a high $V_{oc}$ is anticipated.

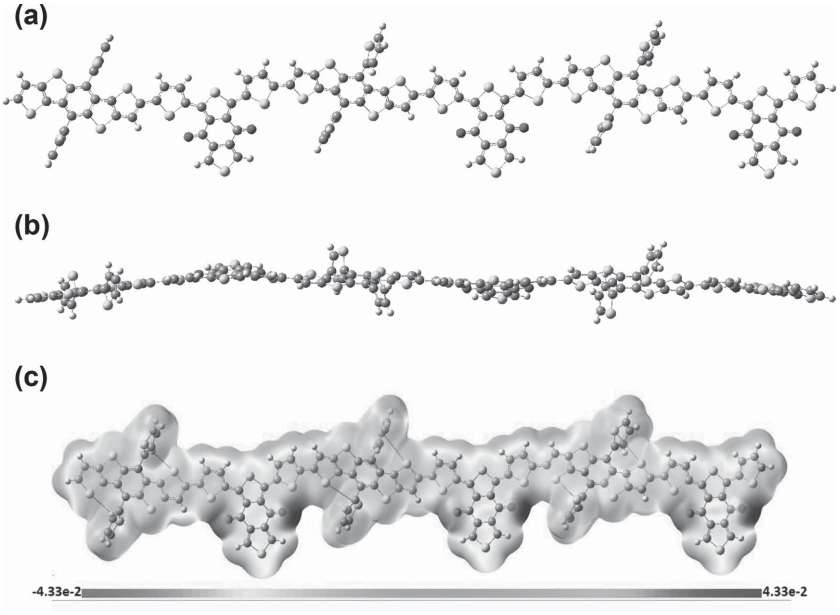


**Figure 1.** Optimized geometries of PDBT-T1 by DFT at the B3LYP/6–31G(d,p) level. a) Side view; b) top view; c) map of the DFT electrostatic potential (ESP) surfaces, dark color indicates greater negative charge, while white and grey colors indicate positive charges.

Carrier transport in pristine PDBT-T1 was investigated using bottom-contact organic field-effect transistors (OFETs). PDBT-T1 was dissolved in $CHCl_3$ and then spin cast on top of octadecyltrichlorosilane (OTS)-treated $SiO_2$/Si substrates with prepatterned Ti/Au electrode. Typical output and transfer curves are presented in Figure S3, Supporting Information. As can be seen from its transfer curve, the device shows typical p-type transport. The hole mobility was estimated to be ≈0.03 $cm^2\ V^{-1}\ s$ and the on/off ratio is about $2 \times 10^6$. In comparison with highest values reported for D–A conjugated polymeric donors,[16] PDBT-T1 shows a moderate hole mobility, which is naturally attributed to the coplanarity of PDBT-T1 backbone and should be beneficial in realizing high performance organic solar cells.

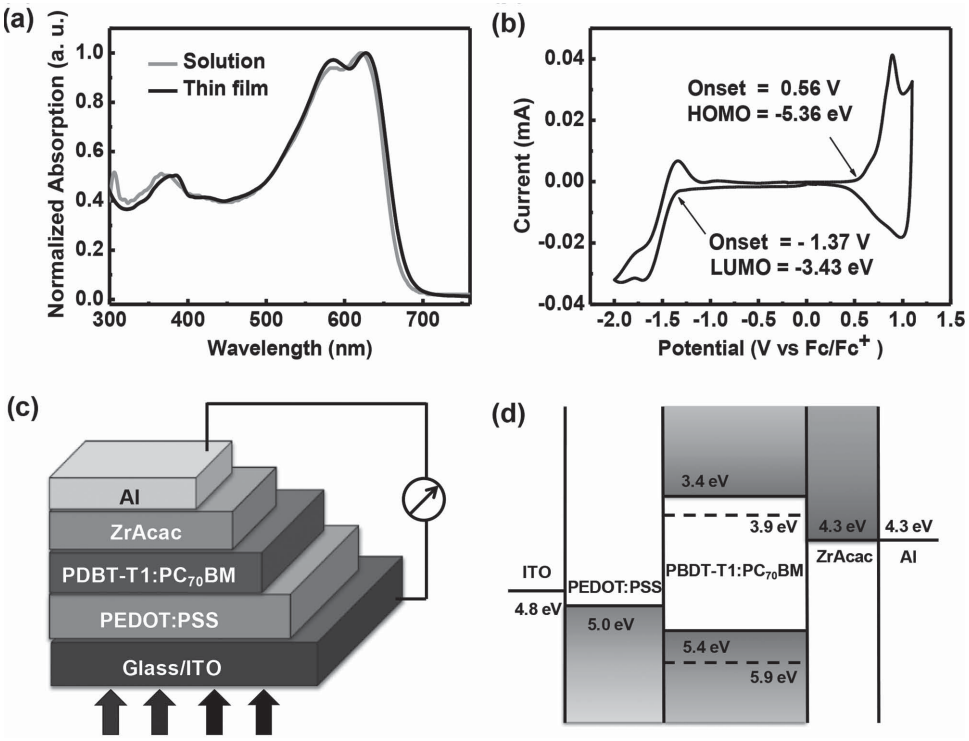


**Figure 2.** a) UV–vis absorption spectra of PDBT-T1 in diluted $CHCl_3$ and thin film. b) The electrochemical cyclic voltammetry measurement of PDBT-T1. The HOMO and LUMO levels calculated from the onset oxidation and reduction potentials are –5.36 and –3.43 eV, respectively. The electrochemical bandgap is estimated to be about 1.93 eV. c) Device structure of organic solar cells used in this study. d) Schematic energy diagram of the components in PDBT-T1:$PC_{70}BM$ solar cells.

To assess the photovoltaic performance of PDBT-T1, BHJ organic solar cells with a conventional architecture were fabricated (Figure 2c). A mixed solution of PDBT-T1 and $PC_{70}BM$ in $CHCl_3$ with different weight ratios was spin cast atop PEDOT:PSS layer to form the active layer. The commercially available zirconium acetylacetonate (ZrAcac), recently demonstrated as an efficient cathode interfacial layer (CIL),[17] was chosen as the CIL, and inserted between PDBT-T1/$PC_{70}BM$ active layer and Al electrode. The well matched energy level of ZrAcac layer and Al is helpful for efficient charge extraction. The details of device fabrication procedures are described in the Experimental Section.

The effect of the weight ratios of PDBT-T1/$PC_{70}BM$ on cell performance was first studied. Weight ratios were varied in a large range from 2:1 to 1:3 for PDBT-T1:$PC_{70}BM$ blend films. The current density–voltage (*J*–*V*) curves of devices under simulated AM 1.5 G irradiation with intensity of 100 mW $cm^{-2}$ are shown in Figure S4, Supporting Information. The device parameters are summarized in Table S1, Supporting Information. From the table, it can be seen that the weight ratio plays an important role in determining the device performance. The optimum ratio was found to be around 1:1.

On the basis of a 1:1 blend ratio, PDBT-T1:$PC_{70}BM$ solar cells exhibit high PCEs of 8.35%, with $V_{oc}$ of 0.94 V, $J_{sc}$ of 13.20 mA $cm^{-2}$, and FF 67.3%. Note that the high efficiency of 8.35% is obtained for cells without solvent additives and post-annealing treatments. The commonly used processing additive, DIO, was employed to further improve the efficiency. Photovoltaic performance of the devices based on PDBT-T1:$PC_{70}BM$ (1:1, w/w) with different DIO additive contents are summarized in **Table 1**. The current density–voltage (*J*–*V*) characteristics of solar cells under simulated AM 1.5 G irradiation with intensity of 100 mW $cm^{-2}$ are shown in **Figure 3**. When 1% v/v DIO was added to the blend solution, solar cells show PCEs of 8.50%, which is comparable to the efficiency of cells without using DIO additive. Interestingly, we found that decreasing the DIO concentration leads to a significant improvement in device performance. The peak efficiency was achieved at 0.5% v/v DIO. The champion device yielded a high PCE of 9.74%, with $V_{oc}$ of 0.92 V, $J_{sc}$ of 14.11 mA $cm^{-2}$, and *FF* of 75.0%. To the best of our knowledge, this efficiency represents the highest values reported in the literature so far for single-junction organic solar

**Table 1.** Photovoltaic performance of solar cells based on PDBT-T1:$PC_{70}BM$ (1:1, w/w) with different DIO additive contents in a conventional structure under the illumination of AM1.5G, 100 mW/$cm^2$.

| DIO [v/v] | $V_{oc}$ [V] | $J_{sc}$ [mA $cm^{-2}$] | FF [%] | PCE[a] [%] |
|---|---|---|---|---|
| 0% | 0.94 | 13.20 | 67.3 | 8.35 (8.01) |
| 0.2% | 0.88 | 13.56 | 73.6 | 8.78 (8.58) |
| 0.5% | 0.92 | 14.11 | 75.0 | 9.74 (9.41) |
| 0.7% | 0.91 | 13.99 | 74.5 | 9.48 (9.28) |
| 1.0% | 0.89 | 13.17 | 72.5 | 8.50 (8.26) |

[a]The values in parentheses are average efficiencies from 20 devices.

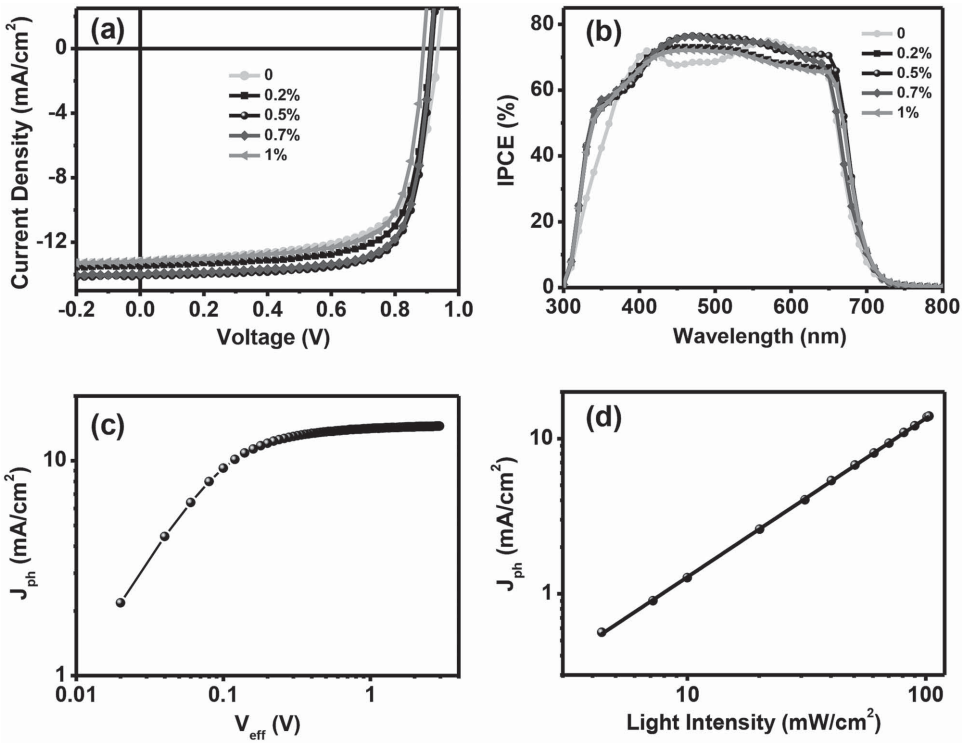


**Figure 3.** a) *J–V* curves of PDBT-T1:$PC_{70}BM$ solar cells (1:1, w/w) with different DIO concentration under the illumination of AM1.5G, 100 mW cm$^{-2}$. b) IPCE plots of PDBT-T1:$PC_{70}BM$ solar cells (1:1, w/w) with different DIO concentrations. c) Photocurrent density ($J_{ph}$) versus effective voltage ($V_{eff}$) characteristics of PDBT-T1:$PC_{70}BM$ solar cells (1:1, w/w) fabricated with 0.5% v/v DIO. d) $J_{ph}$ versus light intensity of PDBT-T1:$PC_{70}BM$ solar cells (1:1, w/w) fabricated with 0.5% v/v DIO.

cell based on WBG polymers. The average efficiency was 9.4% from 20 devices (Figure S5, Supporting Information). The average FF was 74.6%, with the highest one reaching ≈76% (Table S2, Supporting Information). Meanwhile, Ca/Al was used as the cathode layer for comparison, which showed relative lower performance with PCE of ≈8.40%, $V_{oc}$ of 0.91 V, $J_{sc}$ of 13.1 mA cm$^{-2}$, and *FF* of 70.3% than cells with ZrAcac/Al layer (Figure S6, Supporting Information). The incident photon conversion efficiency (IPCE) plots of solar cells with different DIO contents are displayed in Figure 3. All cells show broad IPCE spectra in the 300–700 nm range. IPCE values higher than 70% were observed at 420–650 nm; the maximum value was close to 77% for the champion device, indicating efficient photon harvesting and charge collection within the cell. The $J_{sc}$ calculated from IPCE spectrum was 13.79 mA cm$^{-2}$, which is in good agreement with the $J_{sc}$ obtained from *J–V* curves (14.11 mA cm$^{-2}$) with a 2.3% mismatch.

To understand the main mechanisms involved in the high performance of organic solar cells, the charge generation, extraction properties were studied. We measured the photocurrent density ($J_{ph}$) versus the effective voltage ($V_{eff}$) of the cells. $J_{ph}$ can be defined as $J_{ph} = J_L - J_D$, where $J_L$ and $J_D$ are the photocurrent densities under illumination and in the dark, respectively. $V_{eff}$ can be defined as $V_{eff} = V_0 - V_{bias}$, where $V_0$ is the voltage at which the photocurrent is zero and $V_{bias}$ is the applied external voltage bias.[18] Therefore, $V_{eff}$ determines to the electric field in the bulk region and thereby determines the carrier transport and the photocurrent extraction. At high $V_{eff}$ values, mobile charge carriers rapidly move toward the corresponding electrodes with minimal recombination. It can be seen from Figure 3c, $J_{ph}$ reaches saturation (14.4 mA cm$^{-2}$) at $V_{eff} \geq 2$ V, suggesting that all photogenerated charge carriers are extracted by the electrodes. Under short-circuit condition, $J_{ph}$ is 14.1 mA cm$^{-2}$, which is comparable to that at high $V_{eff}$. Near the maximum power output point, recombination will be strongly competing with the carrier extraction as carriers slow down due to the reduced electric field. However, the $J_{ph}$ of PDBT-T1:$PC_{70}BM$ solar cells (0.5% v/v DIO) is still as high as 12.3 mA cm$^{-2}$ at the maximum power point, ≈86% of all photogenerated carriers collected by the electrodes, indicating efficient photogenerated exciton dissociation and charge collection. We also measured photocurrent ($J_{ph}$) under different light intensities to study the recombination property under the short-circuit condition in PDBT-T1:$PC_{70}BM$ solar cells (Figure 3d). $J_{ph}$ shows a linear dependence on the light intensity with a slope of 1.0, indicative of efficient sweep-out of carriers and weak bimolecular recombination.[19]

To further gain insight into the surface morphology of the BHJ active layer, atomic force microscopy (AFM) was carried out. As shown in **Figure 4**, without DIO additive, PDBT-T1:$PC_{70}BM$ film shows fibrous features with a root mean square (RMS) roughness of 2.02 nm. Upon mixing of 0.5% v/v DIO to the solvent, fibrous features of PDBT-T1:$PC_{70}BM$ film remains unchanged with a RMS of 1.65 nm. The addition of DIO leads to a more uniform blend film with more evenly distributed domains in comparison with the blend film without

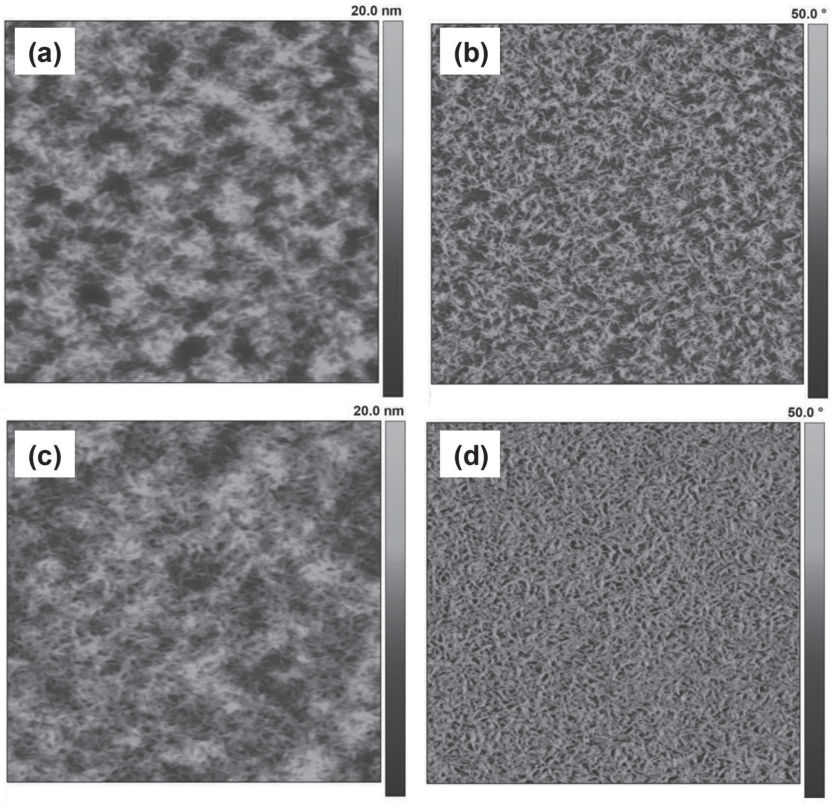


**Figure 4.** AFM topography and phase images for PDBT-T1:$PC_{70}BM$ blend films (1:1, w/w) a,b) without solvent additive and c,d) with 0.5% v/v DIO. The area is 2 × 2 μm.

DIO, as shown in the corresponding phase images. It has been reported that the nanowire-like fibrils are advantageous for BHJ organic solar cells.[20] Here, the smooth fibrous morphology of PDBT-T1:$PC_{70}BM$ film may be beneficial to the bicontinuous, interpenetrating networks required for efficient charge transport, enabling the high PCEs.

In conclusion, a novel DTBDT-based WBG polymer, PDBT-T1, was developed and applied in organic solar cells. Primary optimization of PDBT-T1/$C_{70}BM$ weight ratios yielded PCE = 8.35%. Solar cells processed with 0.5% v/v DIO exhibit a significant increase in FF (up to 75%), leading to an impressive PCE = 9.74%, which is the highest PCE reported for WBG polymers-based single-junction organic solar cells and among the highest values reported for organic solar cell system so far. This high efficiency is attributed to efficient photogenerated exciton dissociation and charge collection in devices. The comprehensive high photovoltaic performance of PDBT-T1 makes it an outstanding candidate as a WBG material for tandem (or multi-junction) organic solar cells.

## Experimental Section

*Synthesis of Dithieno[2,3-d:2′,3′-d′]benzo[1,2-b:4,5-b′]dithiophene-5,10-dione*: To a solution of 5,10-bis((2-ethylhexyl)oxy)dithieno[2,3-*d*:2′,3′-*d*′]benzo[1,2-*b*:4,5-*b*′]dithiophene (1.2 g, 2 mmol) in 50 mL of acetonitrile was added dropwise of ammonium ceric nitrate (6 mmol, 3.3 g) in 20 mL water solution. The reaction mixture was stirred at room temperature for 1 h and then was poured into 100 mL water. The formed precipitate was filtered, washed with water (2 × 50 mL), methanol (4 × 50 mL). After removal of solvents 0.5 g of dark red solid (75%) was obtained. The solid was then dried under vacuum at 70 °C overnight and used directly in the next step.

*Synthesis of 5,10-bis(5-octylthiophen-2-yl) dithieno[2,3-d:2′,3′-d′]benzo[1,2-b:4,5-b′]dithiophene*: In a 50 mL argon purged flask, *n*-butyllithium (2.5 M, 1.7 mL) was added dropwise to a solution of 2-octylthiophene (0.80 g, 4.1 mmol) in THF (50 mL) at 0 °C. The mixture was then warmed to 50 °C and stirred for about 1.5 h. Subsequently, dithieno[2,3-*d*:2′,3′-*d*′]benzo[1,2-*b*:4,5-*b*′]dithiophene-5,10-dione (0.5 g, 1.5 mmol) was added to the reaction mixture, which was then stirred for 1 h at 50 °C. After cooling the reaction mixture to ambient temperature, a mixture of $SnCl_2{\cdot}2H_2O$ (2.7 g, 12 mmol) in 36% HCl (1 mL) was added and the mixture was stirred for additional 1.5 h, after which it was poured into ice water. The mixture was extracted with diethyl ether (3 × 50 mL), and the organic phases were combined. After removing solvent under vacuum, the residue was purified by flash chromatography on silica gel with hexane as eluent to give 5,10-bis((5-octylthiophen-2-yl)dithieno[2,3-*d*:2′,3′-*d*′]benzo[1,2-*b*:4,5-*b*′]dithiophene as light yellow solid (0.58 g, 56%). $^1$H NMR (400 MHz, $CDCl_3$) $\delta$ 7.42 (d, 2H), 7.30 (d, 2H), 7.24 (d, 2H), 6.94 (d, 2H), 2.94 (t, 4H), 1.78 (m, 4H), 1.68–1.38 (m, 20H), 1.06–0.88 (t, 6H). $^{13}$C NMR (101 MHz, $CDCl_3$) $\delta$ 147.33, 143.77, 139.46, 134.89, 134.07, 130.50, 129.67, 128.81, 126.19, 124.24, 120.21, 31.90, 31.60, 30.31, 29.43, 29.33, 29.29, 22.74, 14.15.

*Synthesis of 5,10-bis((5-octylthiophen-2-yl) dithieno[2,3-d:2′,3′-d′]benzo[1,2-b:4,5-b′]dithiophene-2,7-diyl)bis(trimethylstannane)*: 5,10-bis((5-octylthiophen-2-yl)dithieno[2,3-*d*:2′,3′-*d*′]benzo[1,2-*b*:4,5-*b*′]dithiophene (0.55 g, 0.8 mmol) and 40 mL THF were added into a flask under an inert atmosphere. The solution was cooled down to –78 °C by a nitrogen–acetone bath, and 0.68 mL of *n*-butyllithium (2.5 M, 1.7 mmol) was added dropwise. After being stirred at –78 °C for 1 h, 2.6 mL of trimethylchlorostannane (1.0 M in THF, 2.6 mmol) was added in one portion. The mixture was stirred at this temperature for 30 min and then the cooling bath was removed. The reactant was allowed to warm to room temperature and 1 h later, 50 mL water was added and the mixture was extracted by diethyl ether (2 × 50 mL), and the organic phases were combined. After removing solvent under vacuum, the residue was recrystallized from 50 ml methanol to give 5,10-bis((5-octylthiophen-2-yl)dithieno[2,3-*d*:2′,3′-*d*′]benzo[1,2-*b*:4,5-*b*′]dithiophene-2,7-diyl)bis(trimethylstannane) as white solid. (0.34 g, 42%). $^1$H NMR (400 MHz, acetone) $\delta$ 7.45 (s, 2H), 7.26 (d, 2H), 7.02 (d, 2H), 3.02 (t, 4H), 1.80 (m, 4H), 1.55–1.31 (m, 20H), 0.92 (t, 6H), 0.40 (s, 9H). $^{13}$C NMR (101 MHz, acetone) $\delta$ 146.60, 144.98, 143.63, 140.97, 139.17, 134.59, 129.68, 128.60, 127.23, 126.21, 124.08, 31.91, 31.66, 30.30, 29.43, 29.39, 29.28, 22.72, 14.17, -8.31.

*Synthesis of PDBT-T1*: A mixture of 5,10-bis((5-octylthiophen-2-yl)dithieno[2,3-d:2′,3′-d′]benzo[1,2-b:4,5-b′]dithiophene-2,7-diyl)bis(trimethylstannane) (112 mg, 0.11 mmol), T1 (84 mg, 0.11 mmol), in toluene (8 mL) and DMF (0.5 mL) were purged by argon for 30 min, and then 15 mg of $Pd(PPh_3)_4$ was added. After being purged for another 20 min, the mixture was allowed to reflux for 8 h. After cooled to room temperature the polymer was precipitated in methanol. The crude product was collected by filtration and then purified by washing extracted on a soxhlet's extractor with methanol, hexane in succession. The final product was obtained by precipitating the chloroform solution in methanol as dark blue powder. Anal. Caled for $C_{72}H_{78}O_2S_{10}$ (%): C, 66.73; H, 6.07. Found: C, 65.81; H, 6.34. Weight average molecular weight ($\bar{M}_w$) and polydispersity index (PDI) estimated from GPC are 342 kDa and 1.75, respectively.

*FET Device Fabrication*: FET devices were fabricated in a bottom gate, bottom contact configuration on heavily doped n-type Si substrates as the gate and thermally grown 300 nm $SiO_2$ as the dielectric layer. The source and drain electrodes were patterned using standard photolithography and were formed on $SiO_2$ with 5 nm titanium and 30 nm gold. PDBT-T1 was dissolved in $CHCl_3$ with a concentration of 2.5 mg $mL^{-1}$ and then spin cast on top of octadecyltrichlorosilane (OTS)-treated $SiO_2$/Si substrates at a spin coating rate of 2500 rpm. The device was annealed at 180 °C for 5 min and exhibited the high mobility of ≈0.03 $cm^2$ $V^{-1}$ s. Electrical characterization used a Keithley 4200 semiconductor parametric analyzer. All measurements were performed under ambient conditions.

*Solar Cell Fabrication and Characterization*: Organic solar cells were fabricated with the structure of ITO/PEDOT:PSS/PDBT-T1:$PC_{70}BM$/ZrAcac/Al. The patterned ITO glass substrates were first cleaned with detergent, ultrasonicated in water, acetone, and isopropyl alcohol, and subsequently dried overnight in an oven before use. PEDOT:PSS (Heraeus Clevios P VP A 4083) was spin cast from aqueous solution at 4000 rpm for 40 s (the thickness is about 40 nm), and dried at 150 °C for 10 min in air. A solution of PDBT-T1:$PC_{70}BM$ mixture in $CHCl_3$ with different weight ratio and DIO concentration (the concentration of PDBT-T1 is fixed at 6 mg $mL^{-1}$ for all blend solutions) was spin cast at 1700 rpm for 40 s atop PEDOT:PSS layer to form the active layer. The optimal thickness of PDBT-T1:$PC_{70}BM$ solar cell (1:1 w/w, 0.5% v/v DIO) was ≈100 nm, measured by AFM. A thin layer of ZrAcac in ethanol with a concentration of 1.4 mg $mL^{-1}$ was spin cast atop the active layer at a spin coating rate of 3500 rpm. Finally, an aluminum layer (100 nm) at the vacuum condition of $5 \times 10^{-5}$ Pa was deposited by thermal evaporation method. The active area of the devices was 4.50 $mm^2$. During the measurement, an aperture with the area of 3.14 $mm^2$ was used to block stray light. Current density-voltage (*J*–*V*) characteristics were measured using a Keithley 2400 Source Measure Unit. Solar cell performance used an Air Mass 1.5 Global (AM 1.5 G) solar simulator (Class AAA solar simulator, Model 94063A, Oriel) with an irradiation intensity of 100 mW $cm^{-2}$, which was measured by a calibrated silicon solar cell and a readout meter (Model 91150V, Newport). IPCE spectra were measured by using a QEX10 Solar Cell IPCE measurement system (PV measurements, Inc.).

*Instrumentation*: Atomic force microscopy (AFM) images were obtained using a NanoMan VS microscope in the tapping mode. UV–vis absorption measurements were carried out on a Hitachi (model U-3010) UV–vis spectrophotometer. TGA measurements were performed on a Perkin-Elmer Pyris 1 thermogravimetric analyzer. DSC measurements were performed using a Mettler differential scanning calorimeter (DSC822e). Theoretical calculations using DFT were performed using the Gaussian03 package at the B3LYP level of theory with a basis set of 6–31G(d,p). Cyclic voltammetric (CV) measurements were carried out in a conventional three-electrode cell using a platinum plate as the working electrode, a platinum wire as the counter electrode, and $Ag/Ag^+$ electrode as the reference electrode on a Zahner IM6e Electrochemical Workstation in a tetrabutylammonium hexafluorophosphate ($Bu_4NPF_6$) (0.1 M) acetonitrile solution at a scan rate of 20 mV $s^{-1}$.

## Supporting Information

Supporting Information is available from the Wiley Online Library or from the author.

## Acknowledgements

L.H. and T.L. contributed equally to this work. This work was financially supported by the National Natural Science Foundation of China (NSFC) (Grant Nos. 51273203 and 51261160496), the International Science & Technology Cooperation Program of China (Grant No. 2014DFA52820), the 111 project (B14009), and the Fundamental Research Funds for the Central Universities (YWF-14-HXXY-014). The authors thank Prof. Lei Jiang for many fruitful discussions. The authors thank Prof. Donghui Wei and Prof. Mingsheng Tang (Zhengzhou University) for assistance in performing Gaussian DFT calculations. Y.S. gratefully acknowledges Prof. Yunqi Liu (ICCAS) for the assistance with AFM and OFETs measurements.

Received: February 6, 2015
Revised: March 11, 2015
Published online: April 2, 2015

[1] a) J. B. You, L. T. Dou, K. Yoshimura, T. Kato, K. Ohya, T. Moriarty, K. Emery, C. C. Chen, J. Gao, G. Li, Y. Yang, *Nat. Commun.* **2013**, *4*, 1446. b) Y. H. Liu, J. B. Zhao, Z. K. Li, C. Mu, W. Ma, H. Hu, K. Jiang, H. R. Lin, H. Ade, H. Yan, *Nat. Commun.* **2014**, *5*, 5293; c) S. H. Liao, H. J. Jhuo, P. N. Yeh, Y. S. Cheng, Y. L. Li, Y. H. Lee, S. Sharma, S. A. Chen, *Sci. Rep.* **2014**, *4*, 6813; d) A. R. M. Yusoff, D. Kim, H. P. Kim, F. K. Shneider, W. J. Silva, J. Jang, *Energy Environ. Sci.* **2015**, *8*, 303; e) J. Y. You, C. C. Chen, Z. R. Hong, K. Yoshimura, K. Ohya, R. Xu, S. L. Ye, J. Gao, G. Li, Y. Yang, *Adv. Mater.* **2013**, *25*, 3973; f) S. H. Park, I. Shin, K. H. Kim, R. Street, A. Roy, A. J. Heeger, *Adv. Mater.* **2015**, *27*, 298; g) Z. Zheng, S. Q. Zhang, M. J. Zhang, K. Zhao, L. Ye, Y. Chen, B. Yang, J. H. Hou, *Adv. Mater.* **2015**, *27*, 1189; h) H. Q. Zhou, Y. Zhang, C. K. Mai, S. D. Collins, G. C. Bazan, T.-Q. Nguyen, A. J. Heeger, *Adv. Mater.* **2015**, *27*, 1767; i) J. D. Chen, C. H. Cui, Y. Q. Li, L. Zhou, Q. D. Ou, C. Li, Y. F. Li, J. X. Tang, *Adv. Mater.* **2015**, *27*, 1035.

[2] a) H. X. Zhou, L. Q. Yang, W. You, *Macromolecules* **2012**, *45*, 607; b) Y. J. Cheng, S. H. Yang, C. S. Hsu, *Chem. Rev.* **2009**, *109*, 5868; c) Y. F. Li, *Acc. Chem. Res.* **2012**, *45*, 723.

[3] a) H. Neugebauer, N. S. Sariciftci, *Chem. Rev.* **2007**, *107* ,1324; b) P. M. Beaujuge, J. M. J. Frechet, *J. Am. Chem. Soc.* **2011**, *133*, 20009; c) X. Guo, M. Baumgarten, K. Müllen, *Prog. Polym. Sci.* **2013**, *38*, 1832; d) S. Günes, G. Li, R. Zhu, Y. Yang, *Nat. Photonics* **2012**, *6*, 153;

[4] a) Z. C. He, C. M. Zhong, S. J. Su, M. Xu, H. B. Wu, Y. Cao, *Nat. Photonics* **2012**, *6*, 591; b) Y. Y. Liang, Z. Xu, J. B. Xia, S.-T. Tsai, Y. Wu, G. Li, C. Ray, L. P. Yu, *Adv. Mater.* **2010**, *22*, E135; c) L. J. Huo, S. Q. Zhang, X. Guo, F. Xu, Y. F. Li, J. H. Hou, *Angew. Chem. Int. Ed.* **2011**, *50*, 9697; d) T. L. Nguyen, H. Choi, S. J. Ko, M. A. Uddin, B. Walker, S. Yum, J.-E. Jeong, M. H. Yun, T. J. Shin, S. Hwang, J. Y. Kim, H. Y. Woo, *Energy Environ. Sci.* **2014**, *7*, 3040; e) Y. H. Chao, J. F. Jheng, J. S. Wu, K. Y Wu, H. H. Peng, M. C. Tsai, C. L. Wang, Y. N. Hsiao, C. L. Wang, C. Y. Lin, C. S. Hsu, *Adv. Mater.* **2014**, *26*, 5205; f) I. Osaka, T. Kakara, N. Takemura, T. Koganezawa, K. Takimiya, *J. Am. Chem. Soc.* **2013**, *135*, 8834; g) M. J. Zhang, Y. Gu, X. Guo, F. Liu, S. Q. Zhang, L. J. Huo, T. P. Russell, J. H. Hou, *Adv. Mater.* **2013**, *25*, 4944; h) J. Subbiah, B. Purushothaman, M. Chen, T. S. Qin, M. Gao, D. Vak, F. H. Scholes, X. W. Chen, S. E. Watkins, G. J. Wilson, A. B. Holmes, W. W. H. Wong, D. J. Jones, *Adv. Mater.* **2015**, *27*, 702; i) C. E. Small, S. Chen, J. Subbiah, C. M. Amb, S. W. Tsang, T. H. Lai, J. R. Reynolds, F. So, *Nat. Photonics* **2012**, *6*, 115; j) H. X. Zhou, L. Q. Yang, A. C. Stuart, S. C. Price, S. B. Liu, W. You, *Angew. Chem. Int. Ed.* **2011**, *50*, 2995; k) X. G. Guo, N. J. Zhou, S. J. Lou, J. Smith, D. B. Tice, J. W. Hennek, R. P. Ortiz, J. T. L. Navarrete, S. Y. Li, J. Strzalka, L. X. Chen, R. P. H. Chang, A. Facchetti, T. J. Marks, *Nat. Photonics* **2013**, *7*, 825.

[5] a) W. W. Li, A. Furlan, K. H. Hendriks, M. M. Wienk, R. A. J. Janssen, *J. Am. Chem. Soc.* **2013**, *135*, 5529; b) K. Li, Z. Li, K. Feng, X. Xu, L. Wang, Q. Peng, *J. Am. Chem. Soc.* **2013**, *135*, 13549; c) Y. F. Deng, J. Liu, J. T. Wang, L. L. Liu, W. L. Li, H. K. Tian, X. J. Zhang, Z. Y. Xie, Y. H Geng, F. S. Wang, *Adv. Mater.* **2014**, *26*, 471; d) R. C. Coffin, J. Peet, J. Rogers, G. C. Bazan, *Nat. Chem.* **2009**, *1*,657.

[6] J. B. You, L. T. Dou, Z. R. Hong, G. Li, Y. Yang, *Prog. Polym. Sci.* **2013**, *38*, 1909.
[7] a) L. J. Huo, X. Guo, S. Q. Zhang, Y. F. Li, J. H. Hou, *Macromolecules* **2011**, *44*, 4035; b) Z. Li, Y. Zang, C.-C. Chueh, N. Cho, J. R. Lu, X. Y. Wang, J. Huang, C. Z. Li, J. S. Yu, A. K.-Y. Jen, *Macromolecules* **2014**, *47*, 7407; c) M. T. Dang, L. Hirsch, G. Wantz, *Adv. Mater.* **2011**, *23*, 3597; d) X. Gong, C. Li, Z. Lu, G. Li, Q. Mei, T. Fang, Z. Bo, *Macromol. Rapid Commun.* **2013**, *34*, 1163; e) L. J. Huo, Y. Zhou, Y. F. Li, *Macromol. Rapid Commun.* **2009**, *30*, 925; f) R. Kroon, A. D. d. Z. Mendaza, S. Hmmberger, J. Berggvist, O. Backe, G. C. Faria, F. Gao, A. Obaid, W. Zhang, D. Gedefaw, E. Olsson, O. Inganäs, A. Salleo, C. Müller, M. R. Andersson, *J. Am. Chem. Soc.* **2014**, *136*, 11578; g) M. Liu, Y. M. Liang, P. H. Chen, D. C. Chen, K. K. Liu, Y. C. Li, S. J. Liu, X. Gong, F. Huang, S. J. Su, Y. Cao, *J. Mater. Chem. A.* **2014**, *2*, 321.
[8] a) X. Guo, C. Cui, M. Zhang, L. Huo, Y. Huang, J. Hou, Y. Li, *Energy Environ. Sci.* **2012**, *5*, 7943; b) Y. Sun, C. J. Takacs, S. R. Cowan, J. H. Seo, X. Gong, A. Roy, A. J. Heeger, *Adv. Mater.* **2011**, *23*, 2226; c) Z. Tan, S. Li, F. Wang, D. Qian, J. Lin, J. Hou, Y. Li, *Sci Rep.* **2014**, *4*, 4691.
[9] G. Dennler, M. C. Scharber, T. Ameri, P. Denk, K. Forberich, C. Waldauf, C. J. Brabec, *Adv. Mater.* **2008**, *20*, 579.
[10] a) H. Pan, Y. Wu, Y. Li, P. Liu, B.-S. Ong, S. Zhu, G. Xu, *Adv. Funct. Mater.* **2007**, *17*, 3574; b) C. L. Wang, H. L. Dong, W. P. Hu, Y. Q. Liu, D. B. Zhu, *Chem. Rev.* **2012**, *112*, 2208.
[11] a) J. H. Huang, X. Wang, C. L. Zhan, Y. Zhao, Y. X. Sun, Q. B. Pei, Y. Q. Liu, J. N. Yao, *Polym. Chem.* **2013**, *4*, 2174; b) C. Gao, L. W. Wang, X. Y. Li, H. Q. Wang, *Polym. Chem.* **2014**, *5*, 5200; c) L. J. Huo, J. H. Hou, *Polym. Chem.* **2011**, *2*, 2453.
[12] a) Y. Wu, Z. J. Li, X. Guo, H. L. Fan, L. J. Huo, J. H. Hou, *J. Mater. Chem.* **2012**, *22*, 21362; b) Y. Wu, Z. J. Li, W. Ma, Y. Huang, L. J. Huo, X. Guo, M. J. Zhang, H. Ade, J. H. Hou, *Adv. Mater.* **2013**, *25*, 3449; c) H. J. Son, L. Y. Lu, W. Chen, T. Xu, T. Y. Zheng, B. Carsten, J. Strzalka, S. B. Darling, L. X. Chen, L. P. Yu, *Adv. Mater.* **2013**, *25*, 838.
[13] a) J. S. Wu, S. W. Cheng, Y. J. Cheng, C. S. Hsu, *Chem. Soc. Rev.* **2015**, *44*, 1113; b) Y. F. Deng, J. Liu, J. T. Wang, L. L. Liu, W. L. Li, H. K. Tian, X. J. Zhang, Z. Y. Xie, Y. H Geng, F. S. Wang, *Adv. Mater.* **2014**, *26*, 471; c) Y. Li, K. Yao, H. L. Yip, F. Z. Ding, Y. X. Xu, X. Li, Y. Chen, A. K. Y. Jen, *Adv. Funct. Mater.* **2014**, *24*, 3631; d) Y. X. Xu, C. C. Chueh, H. L. Yip, F. Z. Ding, Y. X. Li, C. Z. Li, X. Li, W. C. Chen, A. K. Y. Jen, *Adv. Mater.* **2012**, *24*, 6356; e) H. J. Yun, Y. J. Lee, S. J. Yoo, D. S. Chung, Y.-H. Kim, S.-K. Kwon, *Chem. Eur. J.* **2013**, *19*, 13242; f) S. Sun, P. Zhang, J. F , Li, Y. K. Li, J. L. Wang, S. J. Zhang, Y. J. Xia, X. J. Meng, D. W. Fan, J. H. Chu, *J. Mater. Chem. A.* **2014**, *2*, 15316.
[14] a) Y. Ie, J. Huang, Y. Uetani, M. Karakawa, Y. Aso, *Macromolecules*, **2012**, *45*, 4564; b) D. Qian, L. Ye, M. Zhang, Y. Liang, L. Li, Y. Huang, X. Guo, S. Zhang, Z. Tan, J. Hou, *Macromolecules* **2012**, *45*, 9611.
[15] Z. H. Chen, P. Cai, J. W. Chen, X. C. Liu, L. J. Zhang, L. F. Lan, J. B. Peng, Y. G. Ma, Y. Cao, *Adv. Mater.* **2014**, *26*, 2586.
[16] L. Bian, E. Zhu, J. Tang, W. Tang, F. Zhang, *Prog Polym Sci.* **2012**, *37*, 1292.
[17] F. Wang, Z. Tan, Y. Li, *Energy Environ. Sci.* **2015**, DOI: 10.1039/C4EE03802A.
[18] P. W. M. Blom, V. D. Mihailetchi, L. J. A. Koster, D. E. Markov, *Adv. Mater.* **2007**, *19*, 1551.
[19] a) I. Riedel, J. Parisi, V. Dyakonov, L. Lutsen, D. Vanderzande, J.-C. Hummelen, *Adv. Funct. Mater.* **2004**, *14*, 38; b) P. Schilinsky, C. Waldauf, C. J. Brabec, *Appl. Phys. Lett.* **2002**, *81*, 3885; c) S. R. Cowan, A. Roy, A. J. Heeger, *Phys. Rev. B* **2010**, *82*, 245207.
[20] a) K. H. Hendriks, G. H. L. Heintges, V. S. Gevaerts, M. M. Wienk, R. A. J. Janssen, *Angew. Chem. Int. Ed.* **2013**, *52*, 8341; b) W. Li, K. H. Hendriks, A. Furlan, W. S. C. Roelofs, M. M. Wienk, R. A. J. Janssen, *J. Am. Chem. Soc.* **2013**, *135*, 18942.